Structural evolution of the $KTa_{0.6}Nb_{0.4}O_3$ alkoxide-based solutions: probing the transition metals local environment by X-ray absorption spectroscopy

Sebastjan Glinšek, Iztok Arčon, Barbara Malič, Alojz Kodre, and Marija Kosec

Jožef Stefan Institute, Jamova 39, SI-1000 Ljubljana, Slovenia

e-mail: sebastjan.glinsek@ijs.si

phone: +38614773414

fax: +38614773887

Sebastjan Glinšek, Barbara Malič

Centre of Excellence SPACE-SI, Aškerčeva cesta 12, SI-1000 Ljubljana, Slovenia

Iztok Arčon

University of Nova Gorica, Vipavska 13, SI-5000 Nova Gorica, Slovenia

Alojz Kodre

Faculty of Mathematics and Physics, University of Ljubljana, Jadranska 19, SI-1000 Ljubljana, Slovenia

Abstract The $KTa_{0.6}Nb_{0.4}O_3$ sols for chemical solution deposition of thin films were prepared from potassium acetate and transition metal ethoxides by the 2-methoxyethanol based route. The local environment of both transition metals after reflux times 1 h, 4 h, 24 h, and 48 h, whereby the crystallization behavior of the films was strongly affected, was monitored by extended X-ray absorption fine structure spectroscopy (EXAFS), at Ta L_3 and Nb K edges. The Ta species existed in the sols as monomers, remaining stable even with prolonged reflux time. The Ta-O-K correlations were confirmed in all cases. In contrast, the Nb-alkoxide formed dimers, with a gradual formation of oligomeric species with prolonged refluxing. The Nb-O-K correlations were present after all reflux times. The number of K neighbours around Nb increased upon refluxing, saturating at 24 h.

Keywords *Potassium Tantalate Niobate, Chemical Solution Deposition, EXAFS, Ferroelectric Solid Solutions*

1 Introduction

Perovskite materials are technologically important because of their piezoelectric, ferroelectric, and dielectric properties, which can be exploited in a wide range of electronic applications. The functional properties of solid solutions, such as $Pb(Zr,Ti)O_3$, $PbMg_{1/3}Nb_{2/3}O_3$-$PbTiO_3$, $(Ba,Sr)TiO_3$, $K(Ta,Nb)O_3$ can be tuned through the composition. Compositional heterogeneities within the material lead to a strong deterioration of the properties, therefore a control of compositional homogeneity during the processing is essential.[1,2]

The paraelectric-ferroelectric transition temperature of $K(Ta,Nb)O_3$ varies by changing the Ta/Nb ratio in the temperature interval from 0 K to 708 K.[3] Ta-rich compositions, with the transition temperatures below the room temperature, can be used in microwave devices, and the $KTa_{0.6}Nb_{0.4}O_3$ composition was considered for such applications, analogous to the widely studied Sr-rich $(Ba,Sr)TiO_3$ solid solutions.[4] The material was studied also as a model ferroelectric solid solution.[5]

The processing of $K(Ta,Nb)O_3$ ceramics and also thin films, remains a challenge. Their dielectric properties deviate from those of single crystals and depend strongly on the processing conditions.[4,6] The discrepancy is attributed to the difficult maintenance of exact A site stoichiometry due to a loss of potassium oxide upon heating, and due to a heterogeneous distribution of Ta and Nb at the B sites of the perovskite lattice. Xu et al.[7] employed extended X-ray absorption fine structure spectroscopy (EXAFS) to investigate the B-site compositional homogeneity of the $K(Ta,Nb)O_3$ powders. The alkoxide-based hydrolytic sol-gel synthesis yielded powders with a uniform Ta/Nb distribution already after heating at 700 °C. However, when the material was intentionally synthesized with a non-uniform distribution of Ta and Nb atoms, such heterogeneities remained even after heating as high as 1000 °C.

By chemical solution deposition (CSD), phase-pure perovskite $K(Ta,Nb)O_3$ thin films were prepared on different single-crystal substrates, such as (100) MgO,[8-10] (100) Pt / (100) MgO,[11] (100) and (110) $SrTiO_3$[10,11], with crystal structures and lattice parameters similar to $K(Ta,Nb)O_3$. To prepare single-phase films on structurally significantly different substrates, such as (100) Si and SiO_2

glass, $KNbO_3$ was employed as a seeding layer.[12] We showed that the single-phase perovskite $KTa_{0.6}Nb_{0.4}O_3$ thin films on polycrystalline Al_2O_3 substrate can be prepared from the alkoxide-based sols by the 2-methoxyethanol based route without any seeding layer. The films, prepared from the 1 h-refluxed sol and heated at 900 °C, consisted of perovskite and pyrochlore phases and had a heterogeneous microstructure. The 240 nm thick phase-pure perovskite films with a homogeneous microstructure were obtained by extending the reflux time to 24 h, whereby also the dielectric permittivity was doubled.[13] The increase of permittivity with increasing the reflux time could be explained by promoted formation of intermetallic bonds, as for example proposed for the case of $PbMg_{1/3}Nb_{2/3}O_3$ thin films by Nagakari et al.[14]

In the present study, we prepared $KTa_{0.6}Nb_{0.4}O_3$ sols from potassium acetate and transition metal alkoxides by the 2-methoxyethanol route with different reflux times, from 1 h to 48 h. We exploited Ta L_3-edge and Nb K-edge EXAFS to determine structural differences in the transition metal local environments in respective sols.

2 Experimental

The 0.5 M sols, with the targeted composition $KTa_{0.6}Nb_{0.4}O_3$, were prepared in a dry inert atmosphere by dissolving potassium acetate (99+ %, Sigma-Aldrich), tantalum ethoxide (99.99 % H. C. Starck), and niobium ethoxide (99.99 % H. C. Starck) in 2-methoxyethanol (99.3+ %, Sigma-Aldrich). After refluxing for 1 h, 4 h, 24 h, or 48 h, the sols were distilled to remove the by-products. The as-obtained sols are denoted as the KTN1, KTN4, KTN24, and KTN48, respectively. A full experimental procedure has been reported elsewhere.[13]

Absorption spectra of the sols were measured at C station of HASYLAB in transmission detection mode, using a (111) Si double-crystal monochromator with ~1.5 eV resolution at the Ta L_3-edge (9881 eV) and 2 eV resolution at Nb K-edge (18986 eV). Higher-order harmonics were efficiently eliminated by detuning the monochromator crystals to 60 % of the rocking curve maximum using a stabilization feedback control. The intensity of the X-ray beam was measured by three consecutive 10 cm long ionization detectors, filled with 140 mbar of Ar, 530 mbar of Kr, and 930 mbar of Kr, respectively, for Ta L_3-edge EXAFS, while for Nb K-edge EXAFs the cells were filled with 940 mbar of Ar, 420 mbar of Kr, and 930 mbar of Kr, respectively. The samples were placed between the first two detectors. Exact energy calibration was obtained by a simultaneous absorption measurement on Ta or Nb foil, inserted between the second and the third ionization detector.

The KTN sols were sealed in thin vacuum-tight plastic bags in a dry inert atmosphere to avoid possible reaction with the atmospheric humidity. The thickness of the liquid bags was adjusted for absorption thickness (μd) of about 2 above the investigated absorption edge. The absorption spectra were measured within the interval from -250 eV to 1100 eV relative to the absorption edge. In the X-ray absorption near edge structure (XANES) region the equidistant energy steps of 0.5 eV were used, while for the EXAFS region the equidistant k-steps ($\Delta k \approx 0.03$ Å^{-1}) were used with an integration time of 1 s/step. To improve the signal-to-noise ratio and to check the stability as well as the reproducibility of the detection system, the data of two identical runs were superposed.

3 Results and discussion

3.1 EXAFS spectra of the sols

The Ta L_3-edge and Nb K-edge EXAFS spectra (Fig. 1) were analysed with the IFEFFIT program package[15]. Distinctive peaks in the Fourier transforms of the EXAFS spectra (Fig. 2) are contributions of the photoelectron backscattering on the near neighbour shells around the central atom, and represent the approximate radial distribution of the atoms surrounding the transition metal atom. A strong compound peak in the R range between 1 Å and 2.4 Å can be attributed to the nearest oxygen neighbours of Ta or Nb atoms. Due to a high signal-to-noise ratio the contributions of more distant Ta and Nb coordination shells up to ~4 Å can be clearly resolved in all spectra. A qualitative comparison of the spectra shows that there are no structural changes around Ta atoms in the sols after different reflux times. On the other hand, significant structural changes are indicated in the Nb environment in the nearest and more distant coordination shells (Fig. 2b).

The quantitative structural information of the local Ta and Nb neighbourhood (type and average number of neighbours, radii and Debye-Waller factors of neighbouring shells) was obtained by EXAFS analysis in which the model EXAFS function was fitted to the measured EXAFS spectra. For the purpose, we constructed model EXAFS functions *ab initio*, from a set of scattering paths of the photoelectron obtained in a tentative spatial distribution of neighbour atoms with the FEFF6 program code[16]. The atomic species of the neighbours were identified in the fit by their specific scattering factors and phase shifts. The model for Ta EXAFS comprised oxygen atoms in the first coordination shell, and carbon and potassium atoms in more distant shells. An additional shell of Nb neighbours had to be introduced for Nb EXAFS spectra.

We introduced three variable parameters for each shell of neighbours: the shell coordination number (N), the distance (R), and the Debye-Waller factor (σ^2). In addition, the common shift of the energy origin, ΔE_0, was allowed to vary. The amplitude reduction factor S_o^2 was fixed to 0.99 for Ta and to 0.80[17] for Nb EXAFS spectra. For the Ta spectra, the fitting was performed in the k range from

3.0 $Å^{-1}$ to 15 $Å^{-1}$, and the *R* range from 1.1 Å to 3.8 Å. and for the Nb spectra in the *k* range of 4.0 $Å^{-1}$ to 15 $Å^{-1}$, and the *R* range from 1.2 Å to 3.9 Å.

To minimize the relatively large uncertainties of coordination numbers and Debye-Waller factor, due to high correlations between these parameters in the fit of each individual spectrum, a simultaneous fit of all Ta spectra, and separately a simultaneous fit of all Nb EXAFS spectra was performed. In the simultaneous relaxation, some of the parameters within the group of spectra were constrained to common values, in particular, for Ta spectra, the common energy shift ΔE_0, the interatomic distances of the corresponding shells of neighbours, and the corresponding Debye-Waller factors, except the parameters of the nearest oxygen shell. In the fit of Nb EXAFS spectra, constraining all these common parameters to the same value for all of the spectra would represent a too rigid model, which could not adequately describe all of the structural differences that appeared for the Nb neighbourhood after different reflux times. In this manner 26 active parameters of the model against 80 independent points were obtained for the fit of Ta spectra and 41 active parameters against 74 independent points for Nb spectra.

A complete list of the best-fit parameters for all of the samples is given in Tables 1 and 2. The quality of the fits is illustrated in Fig. 1 and 2.

3.2 Ta and Nb Local Environments

In all KTN sols the Ta atom is octahedrally coordinated by O atoms, as also found in other studies of Ta-alkoxides.[18,19] Five O atoms are located at 1.956 Å in the KTN1 and KTN4 sols and at a slightly larger distance, i.e. 1.964 Å, after long reflux times. There is an additional contribution of O atoms at 2.36 Å in all cases. Despite the simultaneous fit, the correlation between average occupation number *N* and Debye-Waller factor σ^2 of this neighbour shell remained high; therefore *N* was set to one to obtain the coordination number of six. In more distant shells, one K atom is detected at the distance of 3.59 Å in all sols. Ta-O-K bonds are clearly established by the results of the analysis.

Two shells of carbon atoms, one at 3.12 Å and one broad shell at 3.72 Å are ascribed to different organic groups bonded to Ta. Relatively large uncertainty of the number of C atoms is a consequence of highly correlated *N* and σ^2 in the fit. The unrealistically large number of carbon atoms at 3.72 Å is a consequence of the approximation in EXAFS model, which described the signal at these distances

with a single broad shell of carbon atoms. The models including Ta and/or Nb atoms in the second shell were also tested but the existence of Ta-O-Ta or Ta-O-Nb correlations was excluded by the fit.

In the Nb local environment, the first coordination shell is populated with approximately six O atoms at three different distances. In the KTN1 sol, approximately three O-atoms are present at 1.897 Å. Their distance from the central atom varies with the reflux time and reaches 1.946 Å in the KTN48 sol. One O atom is located at 2.26 Å in all cases. The number was not allowed to vary because of the high correlation with the Debye-Waller factor. Approximately two O atoms are present in all the sols at 2.51 Å. Their value has been tied to the number of O atoms at closer distances to keep the total coordination number of six, as typical for niobium alkoxides.[18,19]

Potassium was identified in all the sols at about 3.60 Å. The average number of K atoms could be determined only with a rather large uncertainty, but a gradual increase of number of K neighbours with increasing the reflux time to 24 h was detected unambiguously. Approximately one Nb atom has been determined at 3.83 Å. Average number of Nb neighbours increases slightly with the reflux time. Again, the Nb-O-Ta correlations were excluded by the fit. Several C atoms were also identified in the Nb neighbourhood at three significantly different distances in the range from 3.10 Å to 4.12 Å. They can be ascribed to different organic groups bonded to Nb.

3.3 Discussion

The nearest neighbourhood of both Ta and Nb consists of six O atoms. The closest O atoms belong to the terminal alkoxide groups, which can be either ethoxide and/or 2-methoxyethoxide, as a product of the transalcoholysis reaction (shown for monomeric alkoxide species):

$$TM(OCH_2CH_3)_5 + xCH_3OCH_2CH_2OH \rightarrow$$

$$TM(OCH_2CH_3)_{5-x}(OCH_2CH_2OCH_3)_x + xCH_3CH_2OH \qquad (1)$$

The reaction takes place already at room temperature.[20] However, according to Sedlar and Sayer [21] the transalcoholysis reaction of Nb-ethoxide is not completed at room temperature, therefore the reaction (1) could proceed also during refluxing, which is in agreement with the observed change of the Nb-O distance from 1.897 Å to 1.946 Å with increasing reflux time. The Ta-O distances did not change significantly at longer reflux times. The solvent could coordinatively bond to Nb via its hydroxy or ether groups.[20]

The Nb neighbourhood is populated with at least one Nb atom at 3.83 Å, which indicates the dimeric structure of Nb-species.[19] A slight increase of the number of Nb-neighbours with increasing reflux time could be explained by thermally activated segregation, resulting in the formation of polynuclear oxoalkoxides.[20] In contrast, Ta alkoxide keeps its monomeric structure in all sols.

The K atoms have been identified in more distant shells of both TMs in all the sols. Potassium can bond to the TM via oxo or acetate bridges, formed by the ester elimination reaction or by the addition reaction, respectively.[20] In the case of Ta, the number of K neighbours does not change with the reflux time and can be set to 1. In contrast, in the Nb environment, the number of K atoms gradually increases from 0.5 to 1.0 in the KTN1 and KTN24 sols. So, longer reflux time favors formation of Nb-O-K bonds.

The relationship between the reflux time of the sols and the phase composition of the powders was reported for $LiNbO_3$ prepared from the ethoxides in ethanol. The bimetallic complex $LiNb(OEt)_6$ was obtained only after prolonged reflux and it served as a "molecular building block" for the crystallization of the phase-pure $LiNbO_3$ powder.[22,23] In our case, the Ta-O-K correlations were established already after one hour of refluxing and did not change with time, while in the Nb case, the K/Nb ratio was saturated only after 24 h of reflux.

4 Summary

EXAFS analysis of Ta and Nb local environment in the 2-methoxyethanol based sols for chemical solution deposition of the $KTa_{0.6}Nb_{0.4}O_3$ thin films was employed to obtain information on correlations between constituent atoms, depending on the time of reflux.

The local environment of Ta atoms is almost independent from the reflux time; it is coordinated by six oxygen atoms in the first shell and potassium atom in the second shell of neighbours. There are no Ta-O-Ta or Ta-O-Nb correlations present in the sols.

In contrast, Nb local environment changes with reflux time. After 1 h of reflux, Nb is present in the form of dimers and the number of the Nb neighbours slightly increases with the reflux time. The Nb-O-K correlations were confirmed already after 1 h, however, a steady state was established only after 24 h of reflux. The formation of bimetallic species between potassium and both transition metals is directly related to the crystallization of $KTa_{0.6}Nb_{0.4}O_3$ thin films on polycrystalline alumina: 24 h of reflux is needed to prepare the perovskite films.[13]

Acknowledgements This work was supported by the Slovenian Research Agency (Program P2-0105; Young Researcher Program, contract number: 10000-07-3100068), the Ministry of Education, Science and Sport of Slovenia, by the European Network of Excellence ´ALISTORE` network, and by DESY and the European Community's Seventh Framework Programme (FP7/2007-2013) ELISA (European Light Sources Activities) under grant agreement n° 226716. Access to synchrotron radiation facilities of HASYLAB (project II-20080058 EC) is acknowledged. We would like to thank Adam Webb, Roman Chernikov and Edmund Welter of HASYLAB, for support and expert advice on beamline operation.

Figures

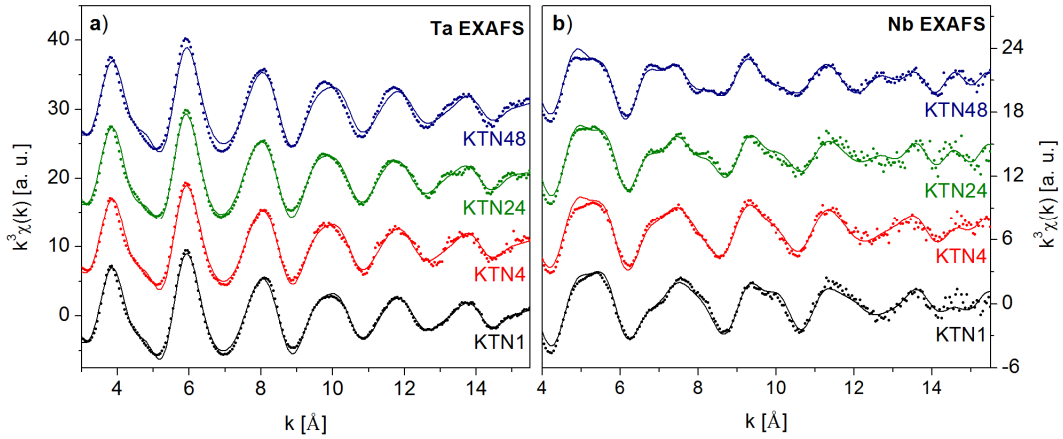

Fig. 1 The k^3-weighted a) Ta and b) Nb EXAFS spectra of KTN1, KTN4, KTN24, and KTN48 sols (dots) in comparison with the best fit EXAFS model (solid lines).

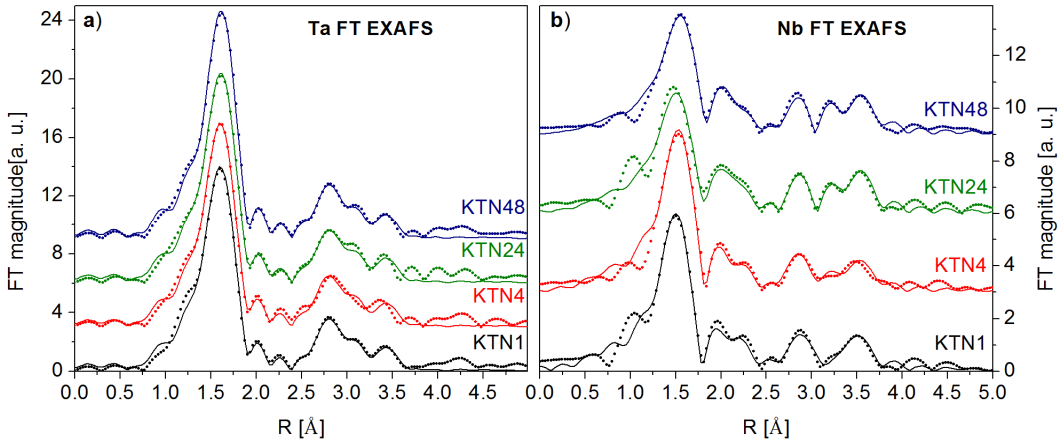

Fig. 2 Fourier transforms of the k^3-weighted a) Ta and b) Nb EXAFS spectra of KTN1, KTN4, KTN24, and KTN48 sols from Fig. 1, calculated in the k-range from 3 Å-1 to 15 Å-1 for Ta, and from 4 Å-1 to 15 Å-1 for Nb EXAFS spectra. Dots – experiment; solid lines – best fit EXAFS model.

Tables

Table 1: Parameters of the nearest coordination shells around Ta in $KTa_{0.6}Nb_{0.4}O_3$ sols after different reflux times: atomic species, average number of the atomic species *N*, distance *r*, and Debye-Waller factor σ^2. The uncertainty of the last digit is given in parentheses.

Sol	Neighbour atom	*N*	*r* [Å]	σ^2[Å^2]
KTN1	O	5.1(1)	1.956(2)	0.0044(2)
	O	1	2.36(2)	0.011(2)
	C	5.2(7)	3.117(5)	0.006(1)
	K	1	3.59(1)	0.0041(7)
	C	17(2)	3.722(7)	0.014(2)
KTN4	O	5.1(3)	1.956(2)	0.0044(2)
	O	1	2.36(2)	0.011(2)
	C	5(1)	3.117(5)	0.006(1)
	K	1	3.59(1)	0.0041(7)
	C	17(4)	3.722(7)	0.014(2)
KTN24	O	5.4(2)	1.964(2)	0.0045(3)
	O	1	2.36(2)	0.011(2)
	C	5(1)	3.117(5)	0.006(1)
	K	1	3.59(1)	0.0041(7)
	C	18(3)	3.722(7)	0.014(2)
KTN48	O	5.4(2)	1.964(2)	0.0036(2)
	O	1	2.36(2)	0.011(2)
	C	5(1)	3.117(5)	0.006(1)
	K	1	3.59(1)	0.0041(7)
	C	18(3)	3.722(7)	0.014(2)

Table 2: Parameters of the nearest coordination shells around Nb in $KTa_{0.6}Nb_{0.4}O_3$ sols after different reflux times: atomic species, average number of the atomic species *N*, distance *r*, and Debye-Waller factor σ^2. The uncertainty of the last digit is given in parentheses.

Sol	Neighbour atom	N	r [Å]	σ^2[Å^2]
KTN1	O	2.4(3)	1.897(4)	0.0032(6)
	O	1.0	2.26(2)	0.008(2)
	O	2.5(3)	2.51(1)	0.011(2)
	C	4(1)	3.101(6)	0.006
	C	8(2)	3.37(1)	0.008
	K	0.5	3.60(1)	0.0018(5)
	Nb	1.2(2)	3.83(1)	0.006
	C	7(3)	4.12(2)	0.01
KTN4	O	2.7(2)	1.922(4)	0.0034(4)
	O	1.0	2.26(2)	0.008(2)
	O	2.3(2)	2.51(1)	0.011(2)
	C	4(1)	3.101(6)	0.006
	C	8(1)	3.37(1)	0.008
	K	0.75	3.60(1)	0.0018(5)
	Nb	1.1(2)	3.83(1)	0.006
	C	6(2)	4.12(2)	0.01
KTN24	O	2.4(4)	1.913(6)	0.005(1)
	O	1.0	2.26(2)	0.008(2)
	O	2.6(4)	2.51(1)	0.009(1)
	C	4(1)	3.101(6)	0.006
	C	8(2)	3.35(1)	0.007
	K	1.0	3.60(1)	0.0018(5)
	Nb	1.6(3)	3.83(1)	0.006
	C	7(2)	4.12(2)	0.01
KTN48	O	2.4(2)	1.946(4)	0.0046(5)
	O	1.0	2.26(2)	0.008(2)
	O	2.6(2)	2.51(1)	0.009(1)
	C	4.0(7)	3.101(6)	0.006
	C	8(1)	3.35(1)	0.007
	K	1.0	3.60(1)	0.0018(5)
	Nb	1.4(2)	3.83(1)	0.006
	C	8(1)	4.12(2)	0.01

References

1. Setter N (ed) (2002) Piezoelectric Materials in Devices. Ceramics Laboratory, Swiss Federal Institute of Technology, Lausanne

2. Tagantsev AK, Sherman VO, Astafiev KF, Venkatesh J, Setter N (2003) J Electroceram 11:5-66

3. Triebwasser S (1959) Physical Review 114:63

4. Sherman V, Venkatesh J, Setter N (2005) J Am Ceram Soc 88:3397-3404

5. Samara GA (2002) MRS Proceedings 718:D8.7

6. DiAntonio CB, Pilgrim SM (2001) J Am Ceram Soc 84:2547-2552

7. Xu J, Wilkinson AP, Pattanaik S (2001) Chem Mater 13:1185-1193

8. Hirano S, Yogo T, Kikuta K, Morishita T, Ito Y (1992) J Am Ceram Soc 75:1701-1704

9. Nazeri A, Kahn M (1992) J Am Ceram Soc 75:2125-2133

10. Suzuki K, Sakamoto W, Yogo T, Hirano S (1999) J Am Ceram Soc 82:1463-1466

11. Kuang AX, Lu CJ, Huang GY, Wang SM (1995) J Cryst Growth 149:80-86

12. Zelezny V, Bursik J, Vanek P (2005) J Eur Ceram Soc 25:2155-2159

13. Glinsek S, Malic B, Vukadinovic M, Kuznik B, Kosec M (2009) Ferroelectrics 387:112-117

14. Nagakari S, Kamigaki K, Nambu S (1996) Jpn J Appl Phys 1 35:4933-4935

15. Ravel B, Newville M (2005) J Synchrotron Radiat 12:537-541

16. Rehr JJ, Albers RC, Zabinsky SI (1992) Phys Rev Lett 69:3397-3400

17. Kodre A, Tellier J, Arcon I, Malic B, Kosec M (2009) J Appl Phys 105

18. Bradley DC, C. MR, P. GD (1978) Metal Alkoxides. Academic Press, London

19. Turova NY, Turevskaya EP, Kessler VG, Yanovksaya MI (2002) The Chemistry of Metal Alkoxides. Kluwer Academic, Boston

20. Brinker CJ, Scherer GW (1990) Sol-gel Science: The Physics and Chemistry of Sol-gel Processing. Academic Press Inc., Boston

21. Sedlar M, Sayer M (1995) J Sol-Gel Sci Techn 5:27-40

22. Hirano SI, Kato K (1987) Adv Ceram Mater 2:142-145

23. Eichorst DJ, Payne DA, Wilson SR, Howard KE (1990) Inorg Chem 29:1458-1459